The Astrophysical Journal, 717:239–244, 2010 July 1 doi:10.1088/0004-637X/717/1/239

SHORT-DURATION GAMMA-RAY BURSTS FROM OFF-AXIS COLLAPSARS

Davide Lazzati[1], Brian J. Morsony[2], and Mitchell C. Begelman[3,4]
[1] Department of Physics, NC State University, 2401 Stinson Drive, Raleigh, NC 27695-8202, USA; davide_lazzati@ncsu.edu
[2] Department of Astronomy, University of Wisconsin-Madison, 5534 Sterling Hall, 475 North Charter Street, Madison, WI 53706-1582, USA
[3] JILA, University of Colorado, 440 UCB, Boulder, CO 80309-0440, USA
[4] Department of Astrophysical and Planetary Sciences, University of Colorado, 391 UCB, Boulder, CO 80309-0391, USA
Received 2009 November 17; accepted 2010 May 19; published 2010 June 9

ABSTRACT

We present two-dimensional (2D) high-resolution hydrodynamic simulations of the relativistic outflows of long-duration gamma-ray burst (GRB) progenitors. We analyze the properties of the outflows at wide off-axis angles, produced by the expansion of the hot cocoon that surrounds the jet inside the progenitor star. We find that the cocoon emission at wide angles may have properties similar to those of the subclass of short-duration GRBs with persistent X-ray emission. We compute the predicted duration distribution, redshift distribution, and afterglow brightness, and we find that they are all in agreement with the observed properties of short GRBs with persistent emission. We suggest that a supernova component, the properties of the host galaxies, and late afterglow observations can be used as a crucial test to verify this model.

Key words: gamma-ray burst: general – hydrodynamics – relativistic processes

Online-only material: color figures

1. INTRODUCTION

Gamma-ray bursts (GRBs) are divided into two classes based on their duration and hardness of their prompt emission spectra (Mazets et al. 1981; Kouveliotou et al. 1993). Long-duration bursts (LGRBs) were the first class for which afterglow observations were possible (Costa et al. 1997). Afterglow observations have allowed us to study them in great detail. We now know that long GRBs are associated with the deaths of massive compact progenitor stars (Woosley 1993; Stanek et al. 2003; Hjorth et al. 2003), take place in compact star-forming galaxies, and can be seen up to redshift $z = 8.2$ (GRB 090423; Tanvir et al. 2009; Salvaterra et al. 2009).

Much less is known about the class of short-duration bursts (SGRBs) and their progenitors. It has been suspected for a long time that SGRB progenitors are binary systems of two compact objects that merge after their orbital energy has been radiated, mostly in gravitational waves (Eichler et al. 1989; Lee & Ramirez-Ruiz 2007; Ramirez-Ruiz & Lee 2009). With the advent of *HETE-2* and *Swift*, afterglow observations of SGRBs have become possible (Fox et al. 2005; Gehrels et al. 2005; Hjorth et al. 2005; Villasenor et al. 2005). The localization of SGRBs has confirmed that some are associated with early-type galaxies and explode at relatively large distances from the center of the host galaxy, confirming their origin as due to the merger of compact objects (Nakar et al. 2007; Berger 2009). However, not all SGRBs fall within such a simple scheme. Some short bursts, especially those showing a plateau of persistent prompt emission in the X-rays (Lazzati et al. 2001; Villasenor et al. 2005) are associated with small, star-forming galaxies, and explode close to the center of their hosts (Troja et al. 2008). This led to the speculation that short bursts have a more diverse family of progenitors than long bursts, possibly involving different compact objects (neutron stars versus black holes; Belczynski et al. 2006; Troja et al. 2008) or transient proto-magnetars (Metzger et al. 2008). Virgili et al. (2009) studied GRB populations based on a new Type I/Type II classification (see Zhang et al. 2007, 2009) and came to the conclusion that most SGRBs closely follow star formation and cannot therefore originate from a traditional merger path. They suggest that a large fraction of SGRBs may be associated with massive stars, analogously to LGRBs. A close association between the progenitors of SGRBs and LGRBs was theoretically explored within the multi-jet scenario (Toma et al. 2005a, 2005b) and in the cannonball scenario (Dado et al. 2009).

In this paper, we show that LGRB progenitors may produce SGRBs at large off-axis angles. This paper is organized as follows: in Section 2, we present our numerical setup, in Section 3, we describe the properties of the relativistic outflow at large off-axis angles, and in Section 4, we discuss some tests that we have performed to assure that this model is consistent with observations of SGRB rates and their afterglows. Our results are summarized and discussed in Section 5.

2. NUMERICAL MODEL

We considered a 16 solar-mass Wolf–Rayet progenitor star, with a pre-explosion radius $R_\star = 4 \times 10^{10}$ cm (Model 16TI; Woosley & Heger 2006). A typical LGRB jet was introduced as a boundary condition at a distance of 10^9 cm from the center of the star, with a constant luminosity $L_{\rm jet} = 5.33 \times 10^{50}$ erg s^{-1}, an initial opening angle $\theta_0 = 10^\circ$, an initial Lorentz factor $\Gamma_0 = 5$, and a ratio of internal over rest mass energy $\eta_0 = 80$, allowing for a maximum Lorentz factor of $\Gamma_\infty = \Gamma_0\eta_0 = 400$, attainable in the case of complete, non-dissipative acceleration. The jet and the progenitor star evolution were computed with the adaptive mesh, special-relativistic hydrodynamic code FLASH (Fryxell et al. 2000) for a total laboratory time of 50 s. The simulation presented here is analogous to the one presented in Morsony et al. (2007) and Lazzati et al. (2009), but was carried out at higher temporal and spatial resolution in order to study short timescale variability properties of GRBs (see Morsony et al. 2010).

We used the results of the simulation to analyze the properties of the outflow at wide angles, larger than 30° off-axis. Figure 1 shows an image in false colors of the asymptotic Lorentz factor Γ_∞ of the outflow at $t = 13.65$ s from the injection of the

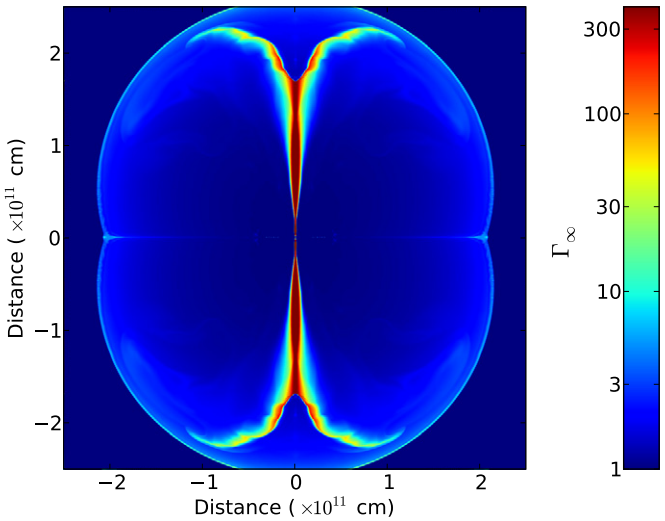

Figure 1. Image of the asymptotic Lorentz factor of the outflow at lab time $t = 13.65$ s from the injection of the jet. The highly relativistic material of the jet is clearly visible along the axis. Moderately relativistic material is also seen along the leading edge of an expanding quasi-isotropic bubble. This is the material that could produce short GRBs.

(A color version of this figure is available in the online journal.)

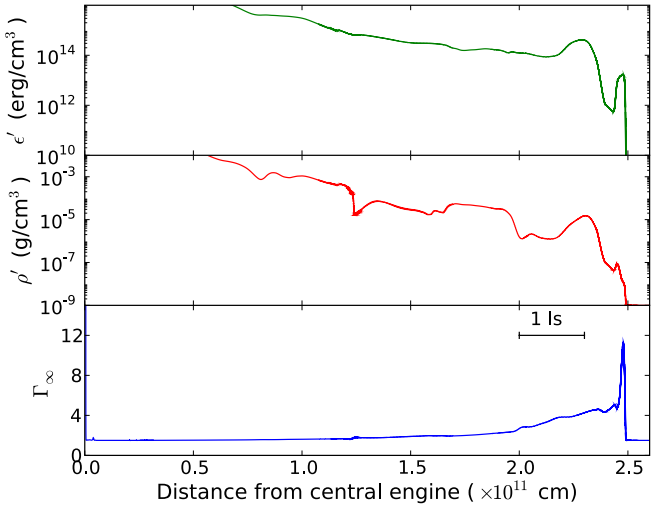

Figure 2. Radial profile of comoving energy density (upper panel), comoving baryon density (middle panel), and asymptotic Lorentz factor (bottom panel) for an off-axis angle $\theta_0 = 45^\circ$. The figure shows that the relativistic component of the cocoon is concentrated on a narrow region at the leading edge, allowing for a very short emission profile. The distance of a light second is indicated in the bottom panel for reference.

(A color version of this figure is available in the online journal.)

jet. The highly relativistic material along the jet axis is clearly visible in dark red. In addition, a thin shell of material with an asymptotic Lorentz factor $\Gamma_\infty \sim 15$ is seen, surrounding the jet out to very wide angles. In the following, we discuss the properties and the potential emission of this shell and show that it can give origin to an SGRB with a persistent tail of low energy emission.

3. OFF-AXIS OUTFLOW PROPERTIES

The propagation of a LGRB jet through its progenitor star is accomplished at the expense of "wasting" some of the jet energy that is recycled into a high pressure cocoon that surrounds the jet (Ramirez-Ruiz et al. 2002a, 2002b; Lazzati & Begelman 2005). Emission from the cocoon has been considered as a source for LGRB precursors (Ramirez-Ruiz et al. 2002a), as an explanation for the steep decay in the early X-ray afterglow (Pe'er et al. 2006), and as a source of seed photons for inverse Compton scattering to explain very high energy components in some LGRBs (Toma et al. 2009). The energy stored in the cocoon is

$$E_{\rm cocoon} = L_{\rm j}\left(t_{\rm br} - \frac{R_\star}{c}\right) \simeq 7.7\times10^{51}\, L_{\rm j,51}\, R_{\star,11}\,{\rm erg}, \quad (1)$$

where $L_{\rm j,51}$ is the jet luminosity in units of 10^{51} erg s^{-1}, $R_{\star,11}$ is the progenitor radius in units of 10^{11} cm, and $t_{\rm br}$ is the breakout time of the jet on the progenitor surface. A jet propagation speed of $v_{\rm head} \simeq 0.3\,c$ has been assumed to compute the numerical value. The simulation we performed, with $t_{\rm br} = 6.2$ s and $R_\star = 4\times10^{10}$ cm, gives $E_{\rm cocoon} = 2.6\times10^{51}$ erg and an average $v_{\rm head} = 0.22\,c$. The cocoon is released approximately at rest on the progenitor surface and, since it is hot and it has high pressure, it subsequently accelerates to relativistic speed, maintaining a constant radial width comparable to the progenitor radius (e.g., Piran 1999). Therefore, should the cocoon be uniform and should it release all its energy into radiation at constant radius, it would produce emission for a duration $\delta t = \delta R/c \sim R_\star/c$, approximately 1 s for our progenitor star.[5]

Figure 2 shows the radial profile of the cocoon comoving energy density, comoving baryon density, and asymptotic Lorentz factor at $\theta_0 = 45^\circ$ and $t = 13.65$ s, when the leading edge of the cocoon has reached a radius $r = 2.5\times10^{11}$ cm, the outer edge of our simulation box. The figure shows that the cocoon develops a radial structure during its expansion and acceleration outside of the star, with a leading shell of relativistic material that has a thickness of only a fraction of a light second. The development of the radial stratification allows for the production of light transients with duration significantly shorter than the light crossing time of the progenitor star.

An important feature of the cocoon outflow is that its Lorentz factor is smaller than the one of the jet material. This is caused by the fact that the internal energy per baryon in the cocoon is less than the internal energy per baryon in the jet. The decrease of internal energy per baryon is due to the combination of two processes. First, part of the cocoon energy is expended in pdV work for creating the cocoon cavity inside the star. Second, the material that forms the cocoon is not purely jet material but is contaminated by mixing with the stellar material. While numerical simulations can very accurately compute the pdV work, it is difficult to calculate the amount of mixing, and therefore the Lorentz factor reported in Figure 2 should be taken with some caution.

4. OBSERVED PROPERTIES OF SHORT GRBs FROM COLLAPSARS

We use the results of our high-resolution simulation to compute observable properties of potential GRBs. First, we compute light power curves. These (see also Morsony et al. 2010) are light curves computed under the assumption that a fraction of the energy in the outflow is converted into radiation

[5] Note that this simplified equation implies that the duration of the transient scales is linearly with the stellar radius. Large stars would therefore produce longer transients that would not be classified as short GRBs.

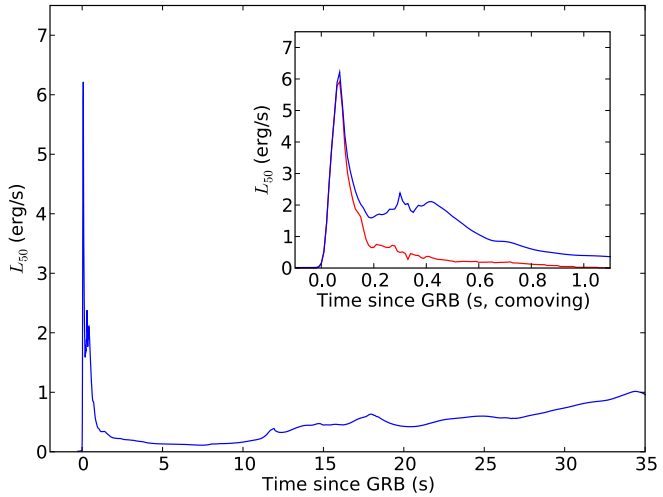

Figure 3. Bolometric light power curve of large off-axis angle GRBs from collapsars. The curve is computed at a distance $R = 2.5 \times 10^{11}$ cm from the GRB engine (the outer edge of the simulation box) at an off-axis angle $\theta_0 = 45°$. As a consequence of the shell dynamic evolution at or beyond the photosphere of the outflow, the real light curve should appear slightly broader (see Section 4 for a discussion of the conditions under which this light curve is accurate). The main panel shows the curve from all the material moving with a minimum bulk Lorentz factor $\Gamma \geqslant 2$. The inset shows a zoom of the initial second of the light power curve, with a red line showing emission from material with $\Gamma \geqslant 10$, likely the high energy component of the burst.

(A color version of this figure is available in the online journal.)

and radiated at a fixed radius. In this paper, we calculate light power curves at $r = 2.5 \times 10^{11}$ cm. This is the largest radius in our simulation. At an off-axis angle of 45°, the fireball at this radius is still optically thick with an optical depth to Thompson scattering $\tau_T \simeq 8$. The flow therefore becomes optically thin only at a radius $R \sim 7 \times 10^{11}$ cm. Due to the increase in the shell thickness with distance, our calculations give reliable light curve properties as long as the emission radius of a real off-axis GRB is lower than $R \sim 2.5 \times 10^{12}$ cm, beyond which both the radial spreading of the shell and the effect of the fireball curvature make the light curve much broader than we calculate. Even though we do not adopt a physical radiation mechanism, we can separate high frequency emission from lower frequency emission under the assumption that the observed peak frequency of the radiation grows monotonically with the bulk Lorentz factor of the emitting material. Even though it may seem natural, this assumption has important consequences. The cocoon shell has a much lower Lorentz factor than the on-axis jet, but the peak frequencies of LGRBs and SGRBs are comparable. We therefore assume implicitly that the radiation mechanism of the cocoon is different from the radiation mechanism of the jet.

Figure 3 shows the light power curve for an off-axis angle $\theta_0 = 45°$. The emission from material moving with $\Gamma \geqslant 2$ is shown in blue, while the emission from material moving at $\Gamma \geqslant 10$ is shown in red in the inset. Under the above assumption for the correlation between photon frequency and bulk Lorentz factor, the red curve shows high energy emission, while the blue curve shows emission components in the X-rays. The light power curves in the figure display all the characteristic features of SGRBs with persistent emission. The initial spike has a duration of ∼0.1 s and is followed by weaker emission at lower frequencies. In this scenario, the emission at $t \sim 30$ s seen in the main panel is due to material moving with lower Lorentz factor behind the leading edge of the cocoon shell. Unfortunately, our simulation did not last long enough to see the decaying part of the persistent emission. Since the persistent emission is due to the continued activity of the inner engine, it is a tunable parameter in our model. A likely assumption is that the duration of the persistent emission should be similar to the duration of observed LGRBs.

We have so far shown that, under some assumptions, the large off-axis angle emission from LGRB progenitors has the properties of SGRBs with persistent emission components. Our simulation results can also be used to predict the ratio between long- and short-duration GRBs and their redshift distributions. To check whether such distributions are in agreement with observations, we have performed a cosmological sampling of bursts produced according to this model. First, we have computed the light power curves at all off-axis angles and divided the luminosity by a factor of 2 to account for a radiative efficiency of 50%. At all off-axis angles, the light power curves were computed at a fixed radius of 2.5×10^{11} cm, and therefore all the caveats discussed above apply to these calculations. We have then generated a sample of 1 million GRBs with random orientation and with a redshift distribution that follows the star formation rate (we used the star formation rate SFR3 of Porciani & Madau 2001) up to redshift 20. Then we have computed the peak luminosity assuming a cosmology with $h = 0.71$, $\Omega_m = 0.27$, and $\Omega_\Lambda = 0.73$. Finally, we have applied a detection threshold of $F_{\rm lim} = 8 \times 10^{-7}$ erg cm^{-2} s^{-1} for the BATSE instrument (Nava et al. 2008).

The left panel of Figure 4 shows the observed T_{50} distribution from our cosmological sampling (blue line).[6] The BATSE duration distribution is overlaid for comparison. Our synthetic T_{50} distribution result shows clearly the broad peak of LGRBs, and a tail that extends in the sub-second durations. The model under-predicts the number of SGRBs, as expected since some SGRBs are associated with binary mergers.[7] The agreement between the synthetic distribution and the BATSE data is only qualitative as a result of the fact that the synthetic distribution is based on a single jet/progenitor configuration, while the real progenitor population is likely characterized by some degree of diversity.

From the same cosmological sampling of our collapsar model, we computed the redshift distribution of both long- and short-duration GRBs. The result is reported in the right panel of Figure 4, where the blue line shows the long GRBs and the red line shows the short ones. Again, the results are in qualitative agreement with observations, with SGRBs detected within a redshift $z_{\rm max} \simeq 1.4$ with an average redshift $\langle z \rangle \simeq 0.8$. LGRBs have instead a maximum redshift $z_{\rm max} \simeq 7$ and an average redshift $\langle z \rangle \simeq 2$. Again, the agreement is not exact since our collapsar simulation cannot reproduce the diversity in progenitor and engine properties. In addition, the numbers mentioned above depend on the efficiency that is adopted in the calculation of the light power curves. If an efficiency lower than 50% is selected, the ratio of long over short GRBs increases, and all the typical redshift values decrease. In any case, the fact that with a single progenitor/jet configuration we can obtain such a close qualitative agreement supports the fact that the orientation-dependent jet–star interaction is responsible, at least in part, for the diversity of GRB light curves.

As a final test, we computed the predicted brightness of the afterglow seen by an observer at large off-axis angles. This is an

[6] T_{50} is the time during which 50% of the fluence is detected, measured from the 25th to the 75th percentiles.

[7] Only 15% of the BATSE short GRBs are from off-axis collapsars, according to this model. The fraction may be higher for *HETE-2* and *Swift* since their sensitivity is biased toward lower photon frequencies.

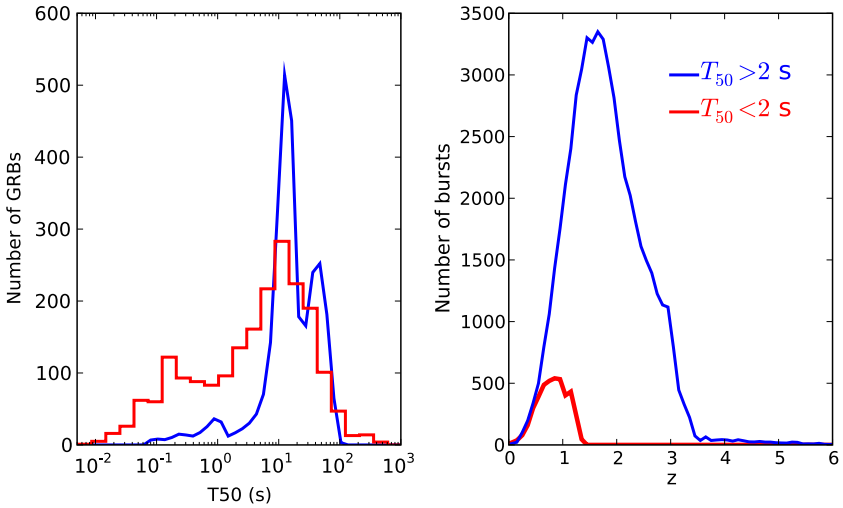

Figure 4. Duration (left) and redshift (right) distributions of GRBs from a cosmological sampling of light power curves from the numerical simulation. In the left panel, the red histogram shows the T_{50} distribution of 2041 BATSE GRBs, while the blue line shows the distribution from the cosmological sampling of our model. The synthetic distribution is normalized to have the same number of long-duration bursts (those with $T_{50} > 2$ s). In the right panel, the synthetic redshift distribution of long and short GRBs is shown. The predicted average redshift of short GRBs is $\langle z \rangle = 0.8$. The maximum observed redshift is $z_{\rm max} = 1.4$. The true redshift distribution may be broader due to the diversity of progenitor and engine properties.

(A color version of this figure is available in the online journal.)

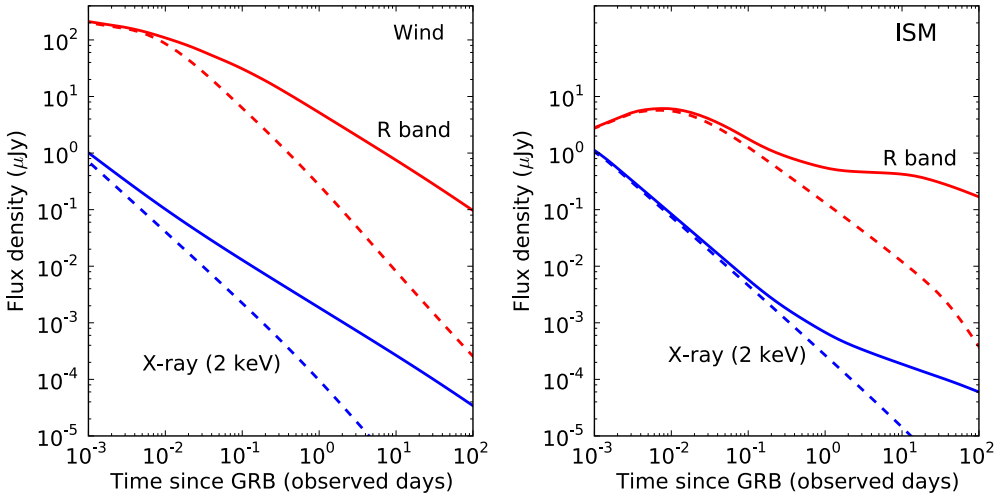

Figure 5. Optical and X-ray afterglow flux density from a burst at $z = 1$ observed at a viewing angle $\theta_0 = 45^\circ$. The left panel shows the afterglow from a wind environment with $A_\star = 1$, while the right panel shows the afterglow from a uniform ISM with $n = 1$. The flattening of the light curves at $t \sim 1$ day is due to the appearance of the bright emission from the on-axis jet and is a characteristic of this model for short GRBs. The dashed lines show an analogous calculation for a uniform shell with the same isotropic equivalent energy of the cocoon shell along the $\theta_0 = 45^\circ$ direction.

(A color version of this figure is available in the online journal.)

important test, since the afterglow at late times will be dominated by the very energetic core of the jet (Rossi et al. 2002, 2004; Zhang & Mészáros 2002). We computed afterglow light curves for an off-axis angle $\theta_0 = 45^\circ$, using the code of Rossi et al. (2004) and assuming no sideways expansion of the jet material (Zhang & MacFadyen 2009). We used equipartition parameters $\epsilon_e = 0.1$ and $\epsilon_B = 0.01$ and a slope $p = 2.3$ for the nonthermal electron population (Panaitescu & Kumar 2001). The afterglow is computed for a wind environment (with $A_\star = 1$) and for a uniform interstellar medium (ISM; $n = 1$ cm^{-3}), and the flux density is computed assuming a redshift $z = 1$. The parameter $A_\star$ is defined through $n(r) = 3 \times 10^{35}\, A_\star\, r^{-2}$, where $n(r)$ is the density of the progenitor wind. $A_\star$ depends on the mass loss rate and wind velocity (see Equation (7) in Panaitescu & Kumar 2001). The results are reported in Figure 5, where a red line shows the R-band afterglow flux density, and a blue line shows the 2 keV flux density. For the wind case, the afterglow has a shallower decay compared to the one from a uniform fireball. For the uniform case, the afterglow is initially identical to the one of a spherical fireball, but at approximately 1 day it flattens, as the bright core of the jet comes into sight.

5. DISCUSSION

We presented the results of numerical simulations of long GRB outflows from massive progenitor stars within the collapsar scenario. In this paper, we focused on the outflow at large off-axis angles, showing that it has a very thin structure and that it can lead to emission with the characteristics of an SGRB. The presence of slower material behind the leading edge of the outflow suggests that the emission at lower frequencies may last longer than the prompt γ-ray emission, a characteristic that has been observed in the subclass of SGRBs with persistent X-ray emission. We propose that at least some SGRBs with persistent

emission are due to collapsars seen at wide angles, 40°–50° away from the axis along which a LGRB is released. We check this possibility by computing the number, the duration distribution, and the redshift distribution of such a short GRB population, finding that the predictions are in good qualitative agreement with observed quantities. A better agreement is prevented by the fact that our simulations do not incorporate the diversity in progenitor and engine populations of LGRBs. Diversity in the properties of the GRB progenitor may also cause a small fraction of short GRBs due to on-axis collapsars with a short-duration engine (Janiuk & Proga 2008; Proga et al. 2009). There are several ways in which the validity of this model can be checked against observations. The smoking gun of an SGRB from an off-axis collapsar would be the detection of an accompanying supernova (SN) explosion in the late afterglow, as observed in LGRBs (Stanek et al. 2003; Hjorth et al. 2003). Such an accompanying SN may however be fairly different from those accompanying LGRBs, due to the difference in the observing angle. In particular, SNe associated with off-axis collapsars should be characterized by slower expansion velocities toward the observer, a less luminous peak (due to the fact that the ^{56}Ni is ejected preferentially along the axis, Maeda et al. 2006), and a longer time to reach maximum. All these characteristic make the SN detection more difficult, and could explain the unsuccessful searches of SN components in several SGRBs[8] (GRB 060505 and GRB 060614; Della Valle et al. 2006; Fynbo et al. 2006; Gal-Yam et al. 2006). Second, if our model is correct, the host galaxies of some SGRBs should have properties fairly similar to those of LGRBs. The comparison of host galaxies of SGRBs and LGRBs shows marked differences (Berger 2009; Fong et al. 2010), especially at low redshift. At $z \sim 1$, the host galaxies of the two populations become more similar (see, e.g., Figure 3 in Berger 2009), as our model would predict. Given the small number of galaxies involved, it is premature to give any firm conclusion, and only further studies with more extensive samples can give better constraints. Along similar lines, Nysewander et al. (2009) found that the density of the ambient medium of LGRB and SGRB afterglows is similar. Finally, SGRBs from off-axis collapsars may be identified through their afterglow properties, especially if they explode in a uniform environment (Figure 5).

The simulation that we have presented is just one case of a big family of possibilities, with diverse progenitors and diverse engine properties. The properties of the SGRBs at large off-axis angles are likely to depend mostly on the luminosity of the jet, with more energetic events from more luminous jets. The volume of the cocoon inside the progenitor star affects instead the temperature and Lorentz factor of the cocoon outflow. Harder SGRBs are therefore expected from more compact stars. Lacking a definite radiative model, however, it is difficult to clearly connect the Lorentz factor of the outflow to a peak frequency of the spectrum. A definitive measurement of a high Lorentz factor ($\Gamma > 100$) for an SGRB would be inconsistent with this model, since the cocoon shell can hardly have Lorentz factors $\Gamma > 20$. Finally, short bursts from off-axis collapsars should have little internal variability, unless some localized dissipation process, such as magnetic reconnection (Lyutikov & Blandford 2003) of relativistic turbulence (Narayan & Kumar 2009), provides the internal energy for the radiation of photons.

In conclusion, we would like to stress that what we presented is a set of necessary conditions for the production of SGRBs. These are by no means sufficient, and at least two important assumptions have to be made to successfully predict SGRBs from our simulation. First, we have to assume that all the radiations are released at a fairly constant and small radius. Should this fail, the light curve would be smeared on a longer time and the burst would not be classified as an SGRB. Second, we have to postulate that the unknown radiation mechanism is able to produce photons in the MeV range, even if it expands at a much slower Lorentz factor compared to the on-axis jet. Should this fail, the cocoon emission would likely produce an X-ray transient rather than an SGRB.

[8] The other explanation being the fact that these bursts are not from off-axis collapsars, given their low redshift.

We thank the anonymous referee for a careful and constructive review, and Giancarlo Ghirlanda for his help with BATSE detection thresholds, and Edo Berger, Massimo della Valle, Asaf Pe'er, Daniel Proga, and Bing Zhang for useful comments. The software used in this work was in part developed by the DOE-supported ASC/Alliance Center for Astrophysical Thermonuclear Flashes at the University of Chicago. This work was supported in part by NASA ATP grant NNG06GI06G and *Swift* GI program NNX06AB69G (M.B.) and NNX08BA92G (D.L.). We thank NASA NAS for the generous allocations of computing time.

REFERENCES

Belczynski, K., Perna, R., Bulik, T., Kalogera, V., Ivanova, N., & Lamb, D. Q. 2006, ApJ, 648, 1110
Berger, E. 2009, ApJ, 690, 231
Costa, E., et al. 1997, Nature, 387, 783
Dado, S., Dar, A., & De Rújula, A. 2009, ApJ, 693, 311
Della Valle, M., et al. 2006, Nature, 444, 1050
Eichler, D., Livio, M., Piran, T., & Schramm, D. N. 1989, Nature, 340, 126
Fong, W., Berger, E., & Fox, D. B. 2010, ApJ, 708, 9
Fox, D. B., et al. 2005, Nature, 437, 845
Fryxell, B., et al. 2000, ApJS, 131, 273
Fynbo, J. P. U., et al. 2006, Nature, 444, 1047
Gal-Yam, A., et al. 2006, Nature, 444, 1053
Gehrels, N., et al. 2005, Nature, 437, 851
Hjorth, J., et al. 2003, Nature, 423, 847
Hjorth, J., et al. 2005, Nature, 437, 859
Janiuk, A., & Proga, D. 2008, ApJ, 675, 519
Kouveliotou, C., Meegan, C. A., Fishman, G. J., Bhat, N. P., Briggs, M. S., Koshut, T. M., Paciesas, W. S., & Pendleton, G. N. 1993, ApJ, 413, L101
Lazzati, D., & Begelman, M. C. 2005, ApJ, 629, 903
Lazzati, D., Morsony, B. J., & Begelman, M. C. 2009, ApJ, 700, L47
Lazzati, D., Ramirez-Ruiz, E., & Ghisellini, G. 2001, A&A, 379, L39
Lee, W. H., & Ramirez-Ruiz, E. 2007, New J. Phys., 9, 17
Lyutikov, M., & Blandford, R. 2003, arXiv:astro-ph/0312347
Maeda, K., Mazzali, P. A., & Nomoto, K. 2006, ApJ, 645, 1331
Mazets, E. P., et al. 1981, Ap&SS, 80, 3
Metzger, B. D., Quataert, E., & Thompson, T. A. 2008, MNRAS, 385, 1455
Morsony, B. J., Lazzati, D., & Begelman, M. C. 2007, ApJ, 665, 569
Morsony, B. J., Lazzati, D., & Begelman, M. C. 2010, ApJ, submitted (arXiv:1002.0361)
Nakar, E. 2007, Phys. Rep., 442, 166
Narayan, R., & Kumar, P. 2009, MNRAS, 394, L117
Nava, L., Ghirlanda, G., Ghisellini, G., & Firmani, C. 2008, MNRAS, 391, 639
Nysewander, M., Fruchter, A. S., & Pe'er, A. 2009, ApJ, 701, 824
Panaitescu, A., & Kumar, P. 2001, ApJ, 554, 667
Pe'er, A., Mészáros, P., & Rees, M. J. 2006, ApJ, 652, 482
Piran, T. 1999, Phys. Rep., 314, 575
Porciani, C., & Madau, P. 2001, ApJ, 548, 522
Proga, D., Janiuk, A., & Moderski, R. 2009, BAAS, 41, 493
Ramirez-Ruiz, E., Celotti, A., & Rees, M. J. 2002b, MNRAS, 337, 1349
Ramirez-Ruiz, E., & Lee, W. 2009, Nature, 460, 1091
Ramirez-Ruiz, E., MacFadyen, A. I., & Lazzati, D. 2002a, MNRAS, 331, 197
Rossi, E., Lazzati, D., & Rees, M. J. 2002, MNRAS, 332, 945
Rossi, E. M., Lazzati, D., Salmonson, J. D., & Ghisellini, G. 2004, MNRAS, 354, 86
Salvaterra, R., et al. 2009, Nature, 461, 1258

Stanek, K. Z., et al. 2003, ApJ, 591, L17
Tanvir, N. R., et al. 2009, Nature, 461, 1254
Toma, K., Wu, X.-F., & Meszaros, P. 2009, arXiv:0905.1697
Toma, K., Yamazaki, R., & Nakamura, T. 2005a, ApJ, 620, 835
Toma, K., Yamazaki, R., & Nakamura, T. 2005b, ApJ, 635, 481
Troja, E., King, A. R., O'Brien, P. T., Lyons, N., & Cusumano, G. 2008, MNRAS, 385, L10
Villasenor, J. S., et al. 2005, Nature, 437, 855
Virgili, F. J., Zhang, B., O'Brien, P., & Troja, E. 2009, arXiv:0909.1850
Woosley, S. E. 1993, ApJ, 405, 273
Woosley, S. E., & Heger, A. 2006, ApJ, 637, 914
Zhang, B., & Mészáros, P. 2002, ApJ, 571, 876
Zhang, B., Zhang, B.-B., Liang, E.-W., Gehrels, N., Burrows, D. N., & Mészáros, P. 2007, ApJ, 655, L25
Zhang, B., et al. 2009, ApJ, 703, 1696
Zhang, W., & MacFadyen, A. 2009, ApJ, 698, 1261